IEEE Control Systems Letters paper presented at
2023 62nd IEEE Conference on Decision and Control (CDC)
December 13-15, 2023. Marina Bay Sands, Singapore

Input Set Design for Active Fault Diagnosis and Control

Feng Xu

Abstract— **This paper first proposes a novel input set design method for set-based active fault diagnosis and then applies it to implement an integrated diagnosis and control scheme. Particularly, taking multiplicative actuator faults as an example, a separation tendency notion is used to characterize the separability of output sets of a group of healthy and faulty modes. At each time instant, an input set is designed for active fault diagnosis by increasing the separation tendency of output sets at the next time instant. Furthermore, an optimal input out of the input set is designed to minimize the output-tracking control error. Based on this logic, integrated active fault diagnosis and control is finally achieved by designing input sets and optimal inputs step by step such that a certain separation tendency is reached for successful diagnosis. At the end, an example is used to illustrate the effectiveness of the proposed method.**

I. Introduction

Set-based active fault diagnosis (AFD) design inputs to excite the system to obtain more information for diagnosis. If healthy and faulty output sets are separated by the inputs, AFD can be guaranteed by testing consistency between outputs and their sets. In principle, AFD has lower conservatism than passive fault diagnosis (PFD). In the literature, there exist some works on set-based AFD. For saving space, only several classical works using zonotopes are introduced. In [2], an input sequence was designed offline for guaranteed AFD by solving a mixed integer quadratic problem based on the separation of all healthy and faulty output zonotopes. In [3], a closed-loop AFD method based on [2] was further proposed. The main shortcoming of the methods in [2] and [3] consists in high computational complexity. Thus, a new notion named set separation tendency instead of set separation conditions used in [2] and [3] was proposed in [7] and [8] to implement AFD with low computational complexity. A detailed survey on both deterministic and stochastic AFD methods can be found in [1].

In active fault-tolerant control (FTC) systems, the objective after diagnosis is to implement FTC to handle faults. However, most of active FTC schemes use PFD. Thus, if AFD is used for FTC, the low conservatism advantage of AFD over PFD can improve the FTC performance. From this viewpoint, integrated design of AFD and control is meaningful. However, there are few works on this topic in the literature [1]. In [10], an FTC scheme was proposed by combining model predictive control (MPC) and the set-based AFD method in [2]. In [4], an FTC scheme was proposed to integrate AFD with MPC by switching the input constraint set of MPC online to a constant AFD input set designed offline by trial and error. In [9], an integrated design of AFD and control was proposed by weighting both AFD and control objectives. In [12], an auxiliary input signal was designed to integrate set-based AFD and control.

This paper is a continuous work of the previous work [4] and aims to propose a novel AFD input set design method based on the real-time system information to replace the previous offline constant input set design method by trail and error, which has potential to improve integrated performance of AFD and control. However, due to the limitation of space, the proposed method is only combined with simple output-tracking control here for integrated AFD and control. However, it is straightforward to combine it with MPC as done in [4]. To help the readers understand the novelties of this paper, the main contributions are summarized as follows:

- A novel AFD input set design method is proposed by formulating and solving a quadratic problem based on the separation tendency of output zonotopes.
- An integrated AFD and control scheme is proposed by designing optimal inputs out of AFD input sets step by step to balance conflicting AFD and control objectives.

Section II introduces preliminary knowledge, the system model and set-based AFD. The main results are presented in Section III. Section IV illustrates the effectiveness of the proposed method. The paper is concluded in Section V.

II. Preliminaries and Problem Formulation

A. Preliminaries

The null and identity matrices are denoted as O and I, respectively. $\mathbf{1}_{m\times n}$ denotes an $(m \times n)$-dimensional matrix full of 1. $\text{diag}(v)$ denotes a diagonal matrix whose diagonal elements are from a vector v. $|\cdot|$ and $\leq$ are understood element-wise. Given $H \in \mathbb{R}^{m\times n}$ with $h_{i,j}$ being the i-th row and j-th column element of H, $\text{vec}(H) = (h_{1,1}, \cdots, h_{m,1}, h_{1,2}, \cdots, h_{m,2}, \cdots, h_{1,n}, \cdots, h_{m,n})^T$.

The Minkowski sum of two sets X and Y is $X \oplus Y = \{x + y \mid x \in X, y \in Y\}$. A zonotope is defined as $Z = g \oplus H\mathbb{B}^m \subset \mathbb{R}^n$ (abbreviated as $Z = \langle g, H\rangle$), where $g \in \mathbb{R}^n$ and $H \in \mathbb{R}^{n\times m}$ are its center and generator matrix, respectively, and $\mathbb{B}^m$ is an m-dimensional unitary box. Given $Z_1 = \langle g_1, H_1\rangle$ and $Z_2 = \langle g_2, H_2\rangle$, $Z_1 \oplus Z_2 = \langle g_1 + g_2, [H_1\ H_2]\rangle$. Given $Z = \langle g, H\rangle$ and an appropriate matrix K, $KZ = \langle Kg, KH\rangle$. The Frobenius radius of $Z = \langle g, H\rangle$ with $H \in \mathbb{R}^{n\times m}$ is the Frobenius norm of H, i.e., $\|Z\|_F = \|H\|_F = \sqrt{\sum_{i=1}^{m} \|h^i\|_2^2}$, where $\|h^i\|_2 = \sqrt{(h^i)^T h^i}$ and h^i is the i-th column of H ([5]).

This work was supported by the National Natural Science Foundation of China (62003186), the Natural Science Foundation of Guangdong, China (2021A1515012628), and the Shenzhen Science and Technology Program, China (JCYJ20210324132606015).

Feng Xu is with Tsinghua Shenzhen International Graduate School, Tsinghua University, 518055 Shenzhen, China (xu.feng@sz.tsinghua.edu.cn).

B. System Model

This paper considers the discrete linear time-invariant (LTI) system under multiplicative actuator faults:

$$x_{k+1} = Ax_k + BG_i u_k + E\omega_k, \tag{1a}$$
$$y_k = Cx_k + F\eta_k, \tag{1b}$$

where $A \in \mathbb{R}^{n_x \times n_x}$, $B \in \mathbb{R}^{n_x \times n_u}$, $C \in \mathbb{R}^{n_y \times n_x}$, $E \in \mathbb{R}^{n_x \times n_\omega}$ and $F \in \mathbb{R}^{n_y \times n_\eta}$ are parameters, k is the k-th discrete time instant, $x_k \in \mathbb{R}^{n_x}$ and $y_k \in \mathbb{R}^{n_y}$ are the state and output, respectively, $u_k \in \mathbb{R}^{n_u}$ is the input, $\omega_k \in \mathbb{R}^{n_\omega}$ is the disturbance, and $\eta_k \in \mathbb{R}^{n_\eta}$ is the noise. $G_i \in \mathbb{R}^{n_u \times n_u}$ is a diagonal matrix used to model the i-th actuator mode, where g_i denotes the i-th diagonal element of G_i. $g_i = 1$ means that the i-th actuator is healthy while $g_i \in [0, 1)$ means that the i-th actuator is faulty. We consider $n_f + 1$ modes (i.e., G_i ($i \in \mathbb{I}_f = \{0, 1, 2, \ldots, n_f\}$), where G_0 is an identity matrix modeling the healthy mode and G_i ($i \neq 0$) models the i-th faulty mode. It is assumed that all the considered modes are detectable and isolable by the proposed method here.

Assumption 2.1: The system matrix A is a Schur matrix.

Assumption 2.2: u_k, ω_k and η_k are bounded by $U = \{u \in \mathbb{R}^{n_u} : |u - u^c| \leq \bar{u}, u^c \in \mathbb{R}^{n_u}\}$, $W = \{\omega_k \in \mathbb{R}^{n_\omega} : \underline{\omega} \leq \omega_k \leq \overline{\omega}\}$ and $V = \{\eta_k \in \mathbb{R}^{n_\eta} : \underline{\eta} \leq \eta_k \leq \overline{\eta}\}$, respectively, where u^c, $\bar{u}$, $\underline{\omega}$, $\overline{\omega}$, $\underline{\eta}$ and $\overline{\eta}$ are constant vectors.

C. Set-Based Fault Diagnosis

Under Assumptions 2.1 and 2.2, corresponding to the i-th actuator mode, a set-based version[1] of (1) is obtained as

$$\hat{X}^i_{k+1} = A\hat{X}^i_k \oplus BG_i u_k \oplus EW, \tag{2a}$$
$$\hat{Y}^i_k = C\hat{X}^i_k \oplus FV, \tag{2b}$$

where $\hat{X}^i_k$ and $\hat{Y}^i_k$ are the state and output sets, respectively. By using zonotopes, (2) is further transformed into

$$\hat{x}^{i,c}_{k+1} = A\hat{x}^{i,c}_k + BG_i u_k + E\omega^c, \tag{3a}$$
$$\hat{H}^{i,x}_{k+1} = [A\hat{H}^{i,x}_k \quad EH_{\bar{\omega}}], \tag{3b}$$
$$\hat{y}^{i,c}_k = C\hat{x}^{i,c}_k + F\eta^c, \tag{3c}$$
$$\hat{H}^{i,y}_k = [C\hat{H}^{i,x}_k \quad FH_{\bar{\eta}}], \tag{3d}$$

where $\hat{x}^{i,c}_k$, ω^c, η^c, $\hat{y}^{i,c}_k$, $\hat{H}^x_k$, $H_{\bar{\omega}}$, $H_{\bar{\eta}}$ and $\hat{H}^y_k$ are the centers and generator matrices of $\hat{X}^i_k$, W, V and $\hat{Y}^i_k$, respectively. Thus, fault diagnosis is done by testing whether or not

$$y_k \in \hat{Y}^i_k, \forall\, i \in \mathbb{I}_f \tag{4}$$

hold online to locate a unique output set satisfying (4). This unique output set finally indicates the current mode.

III. Main Results

A. Analysis of AFD Input Sets

At time instant k, by considering an input set $U^f_k \subseteq U$, a new set-based version of (1) is obtained as

$$X^i_{k+1} = A\hat{X}^i_k \oplus BG_i U^f_k \oplus EW, \tag{5a}$$
$$Y^i_{k+1} = CX^i_{k+1} \oplus FV, \tag{5b}$$

[1]For brevity, this paper follows [2] to use set-wise models. However, the proposed method can be extended to the scheme using set-valued observers.

where X^i_{k+1} and Y^i_{k+1} are the state and output zonotopes, respectively[2]. Then, (5) is transformed into

$$x^{i,c}_{k+1} = A\hat{x}^{i,c}_k + BG_i u^{f,c}_k + E\omega^c, \tag{6a}$$
$$H^{i,x}_{k+1} = [A\hat{H}^{i,x}_k \quad BG_i H^{f,u}_k \quad EH_{\bar{\omega}}], \tag{6b}$$
$$y^{i,c}_{k+1} = CA\hat{x}^{i,c}_k + CE\omega^c + F\eta^c + CBG_i u^{f,c}_k, \tag{6c}$$
$$H^{i,y}_{k+1} = [CA\hat{H}^{i,x}_k \quad CEH_{\bar{\omega}} \quad FH_{\bar{\eta}} \quad CBG_i H^{f,u}_k], \tag{6d}$$

where $x^{i,c}_{k+1}$, $u^{f,c}_k$, $y^{i,c}_{k+1}$, H^x_{k+1}, $H^{f,u}_k$ and H^y_{k+1} are centers and generator matrices of X^i_{k+1}, U^f_k and Y^i_{k+1}, respectively.

When designing an AFD input set $U^f_k \subseteq U$, we could obtain a distribution map of all output sets Y^i_{k+1} ($i \in \mathbb{I}_f$) from (5) to show their separation tendency (i.e., their relative position and size). If designing input sets step by step to enlarge their separation tendency, it is possible to implement fault diagnosis based on (4) at a time instant. The separation tendency of all output sets is affected by two factors:

- The size of output sets.
- The centers distance of output sets.

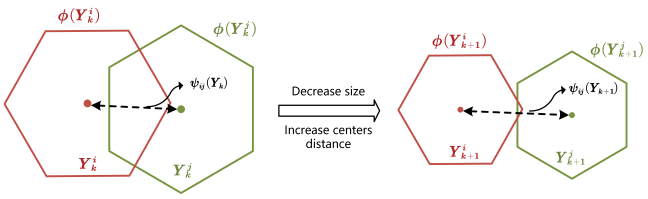

Fig. 1. Separation tendency of two output sets

The center $y^{i,c}_{k+1}$ of Y^i_{k+1} is related to $u^{f,c}_k$ ((6c)) while the Frobenius radius[3] of Y^i_{k+1} is determined by $H^{f,u}_k$ ((6d)). For brevity, we use the square of Frobenius radius of a zonotope to measure its size. Generally, the smaller the size of output sets is and simultaneously the larger their centers distance is, the larger their separation tendency is. A large separation tendency is good for (4) to exclude unmatched modes such that AFD is achieved. In Figure 1, two output sets are used as an example to show the separation tendency, where $\Phi(Y^i_{k+1}) = \|H^{i,y}_{k+1}\|^2_F$ and $\Psi_{ij}(Y_{k+1}) = \|y^{i,c}_{k+1} - y^{j,c}_{k+1}\|^2_2$ denote the size of Y^i_{k+1} and the centers distance of Y^i_{k+1} and Y^j_{k+1}, respectively. However, the objective of this paper is not only to achieve AFD. Instead, it aims to implement simultaneous AFD and control, which includes both AFD and control objectives and can be done by two steps:

- Design an input set at each time instant to increase the separation tendency of output sets for AFD.
- Design an optimal input out of the input set at each time instant for integrated AFD and control.

Thus, an input set plays a key role for both AFD and control, which is a bridge connecting the AFD and control objectives. As shown in Figure 1, the larger the input set is,

[2]The dynamics (2) and (5) are different, where the former is used to implement diagnosis while the latter is used to design an AFD input set.

[3]Since the Frobenius radius of a zonotope has a concise analytical expression, it has advantages to obtain a mathematical formulation of the AFD input set design problem and is used to measure the size of zonotopes.

the larger the output sets are, which implies smaller separation tendency of output sets and lower AFD performance. However, a larger input set implies a larger feasible region for inputs, which can be used to achieve a better control performance. This implies that the size of the input set plays a role to balance the AFD and control objectives.

B. Formulation of Optimization Problem

According to [7], we use the above centers distance and sizes sum to define the separation tendency of Y_{k+1}^i and Y_{k+1}^j $(i \neq j)$ as $S_{k+1}^{ij} = \frac{\Psi_{ij}(Y_{k+1})}{\Phi(Y_{k+1}^i)+\Phi(Y_{k+1}^j)}$. Then, the separation tendency of all n_f+1 output sets is further defined as

$$S_{k+1} = \frac{\sum_{i=0}^{n_f-1}\sum_{j=i+1}^{n_f}\Psi_{ij}(Y_{k+1})}{\sum_{i=0}^{n_f}\Phi(Y_{k+1}^i)}. \tag{7}$$

Based on (7), the design of an AFD input set U_k^f is formulated as an optimization problem:

$$\max_{u_k^{f,c},H_k^{f,u}} \Phi(U_k^f), \text{ s.t. } S_{k+1}-S_k \geq 0, \langle u_k^{f,c}, H_k^{f,u}\rangle \subseteq U, \tag{8}$$

where $\Phi(U_k^f) = \|H_k^{f,u}\|_F^2$ is the size of U_k^f designed to increase the separation tendency of output sets for AFD and simultaneously achieve the maximal size for control.

Proposition 3.1: The constraint[4] $S_{k+1}-S_k \geq 0$ equals

$$\nu_k^T P_{1,k}\nu_k + P_{2,k}\nu_k + P_{3,k} \geq 0, \tag{9}$$

where $\nu_k = [(u_k^{f,c})^T \ (\mathrm{vec}(H_k^{f,u}))^T]^T$ and

$$\hat{e}_k^{ij,x} = \hat{x}_k^{i,c} - \hat{x}_k^{j,c}, e_k^{ij,y} = y_k^{i,c} - y_k^{j,c},$$

$$e_k^y = \sum_{i=0}^{n_f-1}\sum_{j=i+1}^{n_f}\|e_k^{ij,y}\|_2^2, H_k^y = \sum_{i=0}^{n_f}\|H_k^{i,y}\|_F^2,$$

$$P_{1,k} = \begin{bmatrix} P_{1,k}^u & O \\ O & -P_{1,k}^H \end{bmatrix}, \ P_{2,k} = \begin{bmatrix} P_{2,k}^u & O \end{bmatrix},$$

$$P_{3,k} = H_k^y\Big(\sum_{i=0}^{n_f-1}\sum_{j=i+1}^{n_f}(\hat{e}_k^{ij,x})^T A^T C^T CA\hat{e}_k^{ij,x}\Big) -$$
$$e_k^y \mathrm{tr}\Big(\sum_{i=0}^{n_f} CA\hat{H}_k^{x,i}(\hat{H}_k^{x,i})^T A^T C^T +$$
$$(n_f+1)CEH_{\bar{\omega}}(H_{\bar{\omega}})^T E^T C^T + (n_f+1)FH_{\bar{\eta}}H_{\bar{\eta}}^T F^T\Big),$$

$$P_{1,k}^u = H_k^y\Big(\sum_{i=0}^{n_f-1}\sum_{j=i+1}^{n_f}(G_i-G_j)^T B^T C^T CB(G_i-G_j)\Big),$$

$$P_{2,k}^u = 2H_k^y\Big(\sum_{i=0}^{n_f-1}\sum_{j=i+1}^{n_f}(\hat{e}_k^{ij,x})^T A^T C^T CB(G_i-G_j)\Big),$$

$$P_{1,k}^H = e_k^y\Big(I \otimes \Big(\sum_{i=0}^{n_f}(G_i{}^T(CB)^T CBG_i)\Big)\Big).$$

Proof: It is straightforward to obtain the results above by substituting (6) and (7) into $S_{k+1}-S_k \geq 0$. ∎

[4]During AFD, unmatched modes are excluded online. Thus, the number of candidate output sets included in S_{k+1} and S_k may be different. For brevity, we consider that both S_{k+1} and S_k include n_f+1 sets in (9).

Proposition 3.2: Given a generator matrix $H_k^{f,u} \in \mathbb{R}^{n_u\times n_u}$, the constraint[5] $\langle u_k^{f,c}, H_k^{f,u}\rangle \subseteq U$ is equivalent to

$$\Lambda_{1,1}\nu_k + \Lambda_{1,2}|\nu_k| \leq u^c + \bar{u}, \tag{10a}$$
$$\Lambda_{2,1}\nu_k + \Lambda_{2,2}|\nu_k| \leq -u^c + \bar{u}, \tag{10b}$$

where $\Lambda_{1,1} = \begin{bmatrix} I & O \end{bmatrix}$, $\Lambda_{1,2} = \Lambda_{2,2} = \begin{bmatrix} O & LK_{n_u^2\times n_u^2} \end{bmatrix}$, $\Lambda_{2,1} = \begin{bmatrix} -I & O \end{bmatrix}$, $K_{n_u^2\times n_u^2}$ is an $(n_u^2\times n_u^2)$ commutation matrix and[6] $L = \mathrm{diag}([\mathbf{1}_{1\times n_u} \ \mathbf{1}_{1\times n_u}\cdots\mathbf{1}_{1\times n_u}])$.

Proof: Please see the appendix for the proof. ∎

Under Propositions 3.1 and 3.2, (8) is transformed into

$$\max_{\nu_k} \nu_k^T Q\nu_k, \text{ s.t. (9) and (10)}, \tag{11}$$

where $Q = \mathrm{diag}([O \ I])$. Theoretically, an AFD input set U_k^f can be obtained by solving (11). However, due to (9), it is difficult to directly solve (11). Instead, we have to approximate (9) with some conservatism in Section III-C such that an AFD input set can be computed.

C. Design of AFD Input Sets

It is known that (9) is related to the centers distance and size of output sets. As unmatched modes are gradually excluded during AFD, on one hand, the system gradually tends to a steady phase. On the other hand, as AFD succeeds, the number of candidate modes gradually decreases to 1. This implies that the effect of the size of output sets on (9) decreases as AFD proceeds. It is also derived that the indefiniteness of $P_{1,k}$ is induced by $-P_{1,k}^H$ originated from the size of output sets. Following the analysis above, we propose to simplify (9) by a reasonable neglection of the effect of the size of output sets during AFD. In other words, we assume that the total size of candidate output sets changes slowly during AFD (i.e., $\sum_{i=0}^{n_f}\|H_{k+1}^{i,y}\|_F^2 \approx \sum_{i=0}^{n_f}\|H_k^{i,y}\|_F^2$). Based on this idea, (9) is reduced to

$$\nu_k^T\bar{P}_{1,k}\nu_k + \bar{P}_{2,k}\nu_k + \bar{P}_{3,k} \geq 0 \tag{12}$$

with

$$\bar{P}_{1,k}^u = \sum_{i=0}^{n_f-1}\sum_{j=i+1}^{n_f}(G_i-G_j)^T B^T C^T CB(G_i-G_j),$$

$$\bar{P}_{2,k}^u = \sum_{i=0}^{n_f-1}\sum_{j=i+1}^{n_f}2(\hat{e}_k^{ij,x})^T A^T C^T CB(G_i-G_j),$$

$$\bar{P}_{1,k} = \begin{bmatrix} \bar{P}_{1,k}^u & O \\ O & O \end{bmatrix}, \ \bar{P}_{2,k} = \begin{bmatrix} \bar{P}_{2,k}^u & O \end{bmatrix},$$

$$\bar{P}_{3,k} = \sum_{i=0}^{n_f-1}\sum_{j=i+1}^{n_f}(\hat{e}_k^{ij,x})^T A^T C^T CA\hat{e}_k^{ij,x} - e_k^y.$$

In order to match the form of (11), ν_k is also used in (12). Actually, the real variable of (12) should be $u_k^{f,c}$. Thus, $\bar{P}_{1,k}^u$ is generally a positive definite matrix, which means that (12) represents the complementary set of an ellipsoid $\nu_k^T\bar{P}_{1,k}\nu_k + \bar{P}_{2,k}\nu_k + \bar{P}_{3,k} < 0$ (omitting the boundary

[5]$H_k^{f,u}$ is not required to be a square matrix. However, without loss of generality, we consider the case that $H_k^{f,u}$ is square here for brevity.

[6]L is a block diagonal matrix whose diagonal elements are all $\mathbf{1}_{1\times n_u}$.

for brevity). Different from (12), (10) generally forms a polytope. At each time instant, (10) and (12) together mean the intersection of the complementary set of an ellipsoid with a polytope. Besides, in order to compensate the deviation between (9) and (12), a scalar $\gamma_k > 0$ is added to (12), i.e.,

$$\nu_k^T \bar{P}_{1,k} \nu_k + \bar{P}_{2,k} \nu_k + \bar{P}_{3,k} \geq \gamma_k. \tag{13}$$

By giving an appropriate value to γ_k, the deviation between (9) and (12) can be compensated to some extent. Moreover, γ_k affects the AFD performance and the size of the consequent AFD input set. By changing γ_k, on one hand, the AFD performance can be adjusted. On the other hand, the performance of the following integrated AFD and control can be balanced. In this way, (11) is approximated by

$$\max_{\nu_k} \nu_k^T Q \nu_k, \text{ s.t. (10) and (13).} \tag{14}$$

Due to (13), (14) cannot be solved under the convex framework. However, there exists a method in [11] to handle (13) such that (14) is solved. Particularly, the method is a branch and bound method that can search a global solution with a given precision but has high computational complexity. Besides, it is also found that (13) satisfies the constraint requirements of some nonlinear programming solvers such as *fmincon* in Matlab. In order to save space, we turn to *fmincon* and make use of the geometric meaning of the objective function and constraints of (14) to provide a new and simple method to solve (14) in the following.

Particularly, the objective function of (14) means a ball centered at the origin while the feasible region of (14) is an intersection of the complementary set of an ellipsoid with a polytope. Therefore, (14) has the physical meaning to find a point in the intersection to make the ball have the largest size. Moreover, the polytope is fixed and thus only the ellipsoid varies such that the largest ball also varies at different time instants. We use the notations $\mathcal{O}_k$, $\mathcal{E}_k$ and $\mathcal{V}$ to denote the ball (i.e., the objective function), ellipsoid (i.e., the complementary set of (13)) and polytope (i.e., the constraint (10)) at time instant k, respectively. The intersection of $\mathcal{E}_k$ and $\mathcal{V}$ generally has the four possible relations, where the first case is an empty set (e.g., $\mathcal{E}_k$ contains $\mathcal{V}$), the second case is a convex set (e.g., $\mathcal{E}_k$ and $\mathcal{V}$ have no intersection), the third case is a concave set (i.e., $\mathcal{V}$ contains $\mathcal{E}_k$), and the fourth case is also a concave set ($\mathcal{E}_k$ and $\mathcal{V}$ have an intersection but do not contain mutually). Since the second and third cases belong to the same situation, only the second and fourth cases are considered in the following.

First, we analyze the second relation above, where the feasible region of (14) is $\mathcal{V}$ and $\mathcal{O}_k$ reaches its largest size at some vertices of $\mathcal{V}$. Second, we consider the fourth relation above. In this situation, the ball $\mathcal{O}_k$ reaches its largest size at some vertices of $\mathcal{V}$ or at some newly generated vertices of the feasible region by the intersection of $\mathcal{E}_k$ and $\mathcal{V}$. This implies that the vertices of $\mathcal{V}$ play an important role in solving (14).

Because $\mathcal{V}$ is fixed, the first step is to compute the values of the objective function at all vertices of $\mathcal{V}$ offline, i.e., $\Gamma^i = (v^i)^T Q v^i, i \in \mathbb{I}_\mathcal{V} = \{1, 2, \cdots, n_\mathcal{V}\}$, where v^i is the i-th vertex of $\mathcal{V}$, Γ^i is the function value and $\mathbb{I}_\mathcal{V}$ is the index set of all vertices of $\mathcal{V}$. The second step is to test whether some vertices of $\mathcal{V}$ are "bitten" off by the ellipsoid $\mathcal{E}_k$, i.e.,

$$(v^i)^T \bar{P}_{1,k} v^i + \bar{P}_{2,k} v^i + \bar{P}_{3,k} < \gamma_k, i \in \mathbb{I}_\mathcal{V}, \tag{15}$$

where all vertices of $\mathcal{V}$ satisfying (15) are excluded from $\mathbb{I}_\mathcal{V}$ and the index set of all remaining vertices is denoted by $\bar{\mathbb{I}}_\mathcal{V}$. The third step is to choose a vertex in $\bar{\mathbb{I}}_\mathcal{V}$ with the largest objective function value as the initial value of a nonlinear programming solver to solve (14), which assures that the solver can provide a satisfactory solution.

Remark 3.1: Each feasible point of (14) corresponds to a subset of U. Moreover, the subsets of U include three types. The first type represents points inside U. The second type represents degenerated subsets inside U, whose dimensions are smaller than that of U. The third type represents normal subsets inside U, which has the same dimension with U. For the vertices of $\mathcal{V}$ and the solution of (14), we give priority to the points corresponding to the third type of subsets. If there is no third type, give priority to those corresponding to the second type. Otherwise, turn to the first type.

Based on the steps above, an AFD input set is finally designed as $U_k^f = \langle \Lambda_3 \nu_k^*, \text{vec}^{-1}(\Lambda_4 \nu_k^*) \rangle$, where ν_k^* is the solution of (14), $\Lambda_3 = \begin{bmatrix} I & O \end{bmatrix}$, $\Lambda_4 = \begin{bmatrix} O & I \end{bmatrix}$ and $\text{vec}^{-1}(\cdot)$ is the inverse operation of $\text{vec}(\cdot)$.

D. Integrated Design of AFD and Control

After designing U_k^f, all inputs inside U_k^f can be used for AFD. For integrated AFD and control, we only need to select an optimal input out of U_k^f to achieve the best control performance. For brevity, we consider a simple output-tracking problem to introduce the idea. Particularly, when the system is in the i-th mode, a reference output[7] $y_k^{i,ref}$ is given. In this situation, a reference output-tracking error for the j-th output set in the i-th mode is computed as $\tilde{y}_{k+1}^{ij} = y_{k+1}^{i,ref} - \hat{y}_{k+1}^{j,c}$, $i, j \in \mathbb{I}_f$. Since a mode changed from the i-th one is unknown before AFD, the total output-tracking error $\tilde{y}_{k+1}^i$ for all possible output sets is obtained:

$$\tilde{y}_{k+1}^i = \sum_{j=0}^{n_f} \|\tilde{y}_{k+1}^{ij}\|_2^2, \tag{16}$$

where the expression[8] of $\tilde{y}_{k+1}^i$ is obtained by substituting (3a) and (3c) into (16) and is a quadratic function with respect to u_k (omitted here for saving space). Thus, corresponding to the i-th mode, an optimal input u_k^* for integrated AFD and control is obtained by solving a convex problem:

$$u_k^* = \arg \min_{u_k \in U_k^f} \tilde{y}_{k+1}^i. \tag{17}$$

After injecting u_k^* into (1) and (2), the output y_{k+1} and a group of output sets $\hat{Y}_{k+1}^j$ are obtained. Then we employ them for diagnosis by testing (4), where if some output sets violate (4), then they are removed till an AFD decision is finally made at a time instant.

[7]The reference output can be generated by a reference governor designed for an expected output performance.

[8]During AFD, the number of candidate output sets gradually decreases, which means that the sum terms in (16) need to be updated step by step.

IV. Illustrative Example

A four-tank system taken from [6] is used as an example for illustration in this paper. With a sampling time of 10s, the parameters of its linearized discrete-time model are given as $A = \begin{bmatrix} 0.8769 & 0 & 0.0869 & 0 \\ 0 & 0.8581 & 0 & 0.0838 \\ 0 & 0 & 0.9111 & 0 \\ 0 & 0 & 0 & 0.9159 \end{bmatrix}$, $B = \begin{bmatrix} 0.0175 & 0 & 0 \\ 0 & 0.0232 & 0 \\ 0 & 0.0351 & 0.0293 \\ 0.0407 & 0 & 0.0291 \end{bmatrix}$, $C = \begin{bmatrix} 1 & 0 & 0 & 0 \\ 0 & 1 & 0 & 0 \end{bmatrix}$, $E = \begin{bmatrix} 0.7142 & 0.5310 & 0.4978 & 0.2404 \\ 0.3080 & 0.7151 & 0.9360 & 0.6849 \\ 0.6712 & 0.5048 & 0.3893 & 0.8393 \\ 0.6524 & 0.4880 & 0.1171 & 0.9701 \end{bmatrix}$ and $F = \begin{bmatrix} 0.2152 & 0.5100 \\ 0.7603 & 0.4956 \end{bmatrix}$. The disturbances, noises and inputs are bounded by $W = \left\langle \begin{bmatrix} 0 \\ 0 \\ 0 \\ 0 \end{bmatrix}, \begin{bmatrix} 0.001 & 0 & 0 & 0 \\ 0 & 0.001 & 0 & 0 \\ 0 & 0 & 0.001 & 0 \\ 0 & 0 & 0 & 0.001 \end{bmatrix} \right\rangle$, $V = \left\langle \begin{bmatrix} 0 \\ 0 \end{bmatrix}, \begin{bmatrix} 0.001 & 0 \\ 0 & 0.001 \end{bmatrix} \right\rangle$ and $U = \left\langle \begin{bmatrix} 1.5 \\ 1 \\ 2 \end{bmatrix}, \begin{bmatrix} 1 & 0 & 0 \\ 0 & 1 & 0 \\ 0 & 0 & 1 \end{bmatrix} \right\rangle$, respectively. The following actuator modes are considered: $G_0 = \begin{bmatrix} 1 & 0 & 0 \\ 0 & 1 & 0 \\ 0 & 0 & 1 \end{bmatrix}$, $G_1 = \begin{bmatrix} 0.3 & 0 & 0 \\ 0 & 0.95 & 0 \\ 0 & 0 & 0.95 \end{bmatrix}$, $G_2 = \begin{bmatrix} 0.95 & 0 & 0 \\ 0 & 0.3 & 0 \\ 0 & 0 & 0.95 \end{bmatrix}$ and $G_3 = \begin{bmatrix} 0.95 & 0 & 0 \\ 0 & 0.95 & 0 \\ 0 & 0 & 0.3 \end{bmatrix}$. The reference output, initial state and initial state set are given as $y^{ref} = \begin{bmatrix} 0.75 & 0.77 \end{bmatrix}^T$, $x_0 = \begin{bmatrix} 0.75 & 0.77 & 0.84 & 1.08 \end{bmatrix}^T$ and $\hat{X}_0^i = \left\langle \begin{bmatrix} 0.75 \\ 0.77 \\ 0.84 \\ 1.08 \end{bmatrix}, \begin{bmatrix} 0.0001 & 0 & 0 & 0 \\ 0 & 0.0001 & 0 & 0 \\ 0 & 0 & 0.0001 & 0 \\ 0 & 0 & 0 & 0.0001 \end{bmatrix} \right\rangle$, respectively.

The whole simulation includes three different phases. From $k = 0$ to $k = 14$, the system is healthy and the objective of this phase is to implement output-tracking control. This phase is only added to provide a steady period for better illustration of the proposed method. At $k = 15$, the fault G_3 is injected into the system. From $k = 15$ to the AFD time instant $k = k_d$, the proposed method is used to implement AFD and simultaneously suppress the effect of the fault on the output-tracking control performance. From $k = k_d + 1$ to $k = 30$, AFD is done and the fault is already known. The objective of this phase becomes to track the reference output again. The vertices of $\mathcal{V}$ should be first analyzed. In this example, there are three inputs and thus the augmented vector ν_k is 12-dimensional. Moreover, $\mathcal{V}$ has 512 vertices and all their corresponding objective function values[9] can be computed offline as shown in Section III-C. Note that each vertex of $\mathcal{V}$ corresponds to an input set and we could give different priorities to different vertices of $\mathcal{V}$.

During the second phase, $\hat{X}_{15}^1 = \hat{X}_{15}^2 = \hat{X}_{15}^3 = \hat{X}_{15}^0$ and $\gamma_{15} = \gamma_{16} = \gamma_{17} = \gamma_{18} = 0.0002$ are given[10]. Then, AFD input sets are designed as $U_{15}^f = \left\langle \begin{bmatrix} 1.5 \\ 1 \\ 2 \end{bmatrix}, \begin{bmatrix} 0 & 0 & 1 \\ 1 & 0 & 0 \\ 0 & 1 & 0 \end{bmatrix} \right\rangle$, $U_{16}^f = \left\langle \begin{bmatrix} 1.5 \\ 1 \\ 2 \end{bmatrix}, \begin{bmatrix} 0 & 0 & 1 \\ 1 & 0 & 0 \\ 0 & 1 & 0 \end{bmatrix} \right\rangle$, $U_{17}^f = \left\langle \begin{bmatrix} 1.5 \\ 1 \\ 2 \end{bmatrix}, \begin{bmatrix} 0 & 0 & 1 \\ 1 & 0 & 0 \\ 0 & 1 & 0 \end{bmatrix} \right\rangle$ and $U_{18}^f = \left\langle \begin{bmatrix} 1.5 \\ 1 \\ 2 \end{bmatrix}, \begin{bmatrix} 0 & 0 & 1 \\ 1 & 0 & 0 \\ 1 & 0 & 0 \end{bmatrix} \right\rangle$. Using the AFD input sets above and solving (17) at each time instant during the second phase, an input sequence is designed for integrated AFD and control as $u_{15}^* = [2.5,\ 2,\ 2.6042]^T$, $u_{16}^* = [0.5,\ 0,\ 2.3635]^T$, $u_{17}^* = [0.5,\ 0.5939,\ 2.3711]^T$ and $u_{18}^* = [0.5,\ 0.9753,\ 2.3560]^T$,

[9]Since the number of vertices is too large, it is impossible to show all their values and thus they are omitted here for saving space.

[10]At $k = 15$, the proposed method is started and thus the set-based dynamics of all modes should be initialized. We use the state set $\hat{X}_{15}^0$ of the healthy mode for the initialization here. Since $\hat{X}_{15}^0$ is computed online and has a large dimension, it is omitted here for saving space.

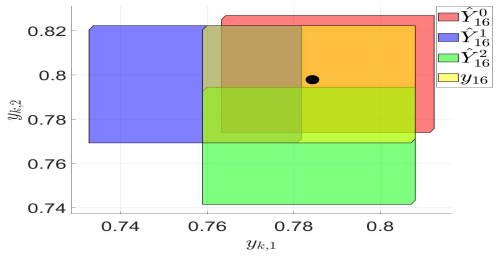

(a) $k = 16$

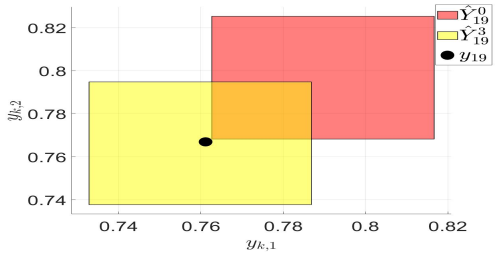

(b) $k = 19$

Fig. 2. Diagnosis of the fault G_3

which is also plotted in Figure 3 for better display. In Figure 3, the notations $u_{k,1}$, $u_{k,2}$ and $u_{k,3}$ denote the first, second and third components of u_k, respectively.

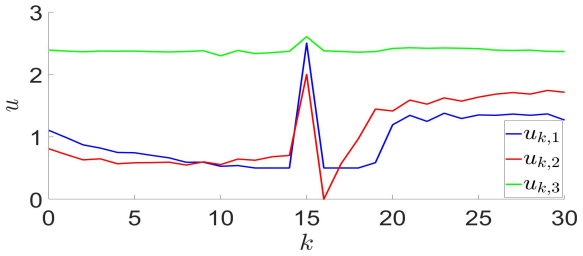

Fig. 3. Designed inputs for the system

The output sets[11] generated by (2) are shown in Figure 2, which are used for diagnosis by testing (4). In Figure 2, $y_k \notin \hat{Y}_{19}^0$ and $y_k \in \hat{Y}_{19}^3$ hold, which implies that the third fault G_3 has been diagnosed at $k_d = 19$. During AFD, the total sizes of output sets are computed as $\sum_{i=0}^{n_f} \|H_{15}^{i,y}\|_F^2 = 0.0036$, $\sum_{i=0}^{n_f} \|H_{16}^{i,y}\|_F^2 = 0.0035$, $\sum_{i=0}^{n_f} \|H_{17}^{i,y}\|_F^2 = 0.0038$ and $\sum_{i=0}^{n_f} \|H_{18}^{i,y}\|_F^2 = 0.0038$, whose differences are small and are negligible in this example as assumed in Section III-C. The output-tracking control is shown in Figure 4, where $y^{ref} = [y_{k,1}^{ref} \quad y_{k,2}^{ref}]^T$, $y_k^* = [y_{k,1}^* \quad y_{k,2}^*]^T$ are the outputs obtained by the proposed method and $y_k = [y_{k,1} \quad y_{k,2}]^T$ are the outputs obtained by injecting a randomly selected input sequence from the AFD input sets for comparison. During the third phase from $k = 19$ to $k = 30$, both the red and blue lines are generated by inputs obtained from $\min_{u_k \in U} \|y_{k+1}^{ref} - \hat{y}_{k+1}^{3,c}\|_2^2$. In Figure 4, the proposed method achieves smoother outputs during AFD, which verifies its effectiveness. The

[11]Only output sets at $k = 16$ and 19 are plotted for saving space.

simulation is done by using Matlab 2019a on a desktop with Intel(R) Core(TM) i7-6700 CPU@3.40GHz and 16GB RAM. The convex problem is solved by the CVX toolbox and the nonlinear problem is solved by the Matlab solver *fmincon*. The average computational time of each step during the first, second and third phases is 0.4580s, 0.6225s and 0.4612s, respectively, which shows that the proposed method is computationally capable.

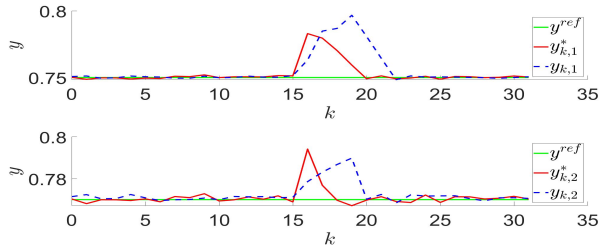

Fig. 4. Output-tracking performance of the proposed method

Remark 4.1: As long as input sets are computed, both AFD and control can be done by solving simple convex problems (17). Particularly, the input sets are mainly involved in two online computations. The first one is related to (15) that is an online function evaluation problem and thus has relatively low complexity. The second one is related to (14) that needs to solve a nonlinear programming problem. Since the proposed method uses nonlinear programming solvers to handle (14), the computational complexity is also acceptable. To illustrate its complexity, the computing time of the example is also given above, which verifies the computational feasibility to implement the proposed method.

V. Conclusions

This paper computes AFD input sets by increasing the separation tendency of all output sets step by step. At each time instant, an AFD input set is obtained by solving an optimization problem. The advantage of designing an AFD input set over an AFD input at each step is that it could be used to simultaneously balance the performances of AFD and control. In the future, the proposed method will be extended to handle more complex systems and more types of faults.

Acknowledgments

Thank Yushuai Wang for the simulations.

References

[1] T.A.N. Heirung and A. Mesbah, Input design for active fault diagnosis, *Annual Reviews in Control*, 47:35 – 50, 2019.

[2] J.K. Scott, R. Findeisen, R.D. Braatz, and D.M. Raimondo, Input design for guaranteed fault diagnosis using zonotopes, *Automatica*, 50(6):1580 –1589, 2014.

[3] D.M. Raimondo, G.R. Marseglia, R.D. Braatz, and J.K. Scott, Closed-loop input design for guaranteed fault diagnosis using set-valued observers, *Automatica*, 74:107– 117, 2016.

[4] F. Xu, S. Olaru, V. Puig, C. Ocampo-Martinez, and S. Niculescu, Sensor-fault tolerance using robust MPC with set-based state estimation and active fault isolation, *International Journal of Robust and Nonlinear Control*, 27(8):1260 – 1283, 2017.

[5] C. Combastel, Zonotopes and Kalman observers: Gain optimality under distinct uncertainty paradigms and robust convergence, *Automatica*, 55:265–273, 2015.

[6] F. Xu, J.B. Tan, Y. Wang, V. Puig and X.Q. Wang, Combining set-theoretic UIO and invariant sets for optimal guaranteed robust fault detection and isolation, *Journal of Process Control*, 78:155-169, 2019.

[7] J.B. Tan, S. Olaru, F. Xu, and X.Q. Wang, Towards a Convex Design Framework for Online Active Fault Diagnosis of LPV Systems, *IEEE Transactions on Automatic Control*, 67(8), 4154-4161, 2022.

[8] F. Xu. Observer-Based Asymptotic Active Fault Diagnosis: A Two-Layer Optimization Framework, *Automatica*, 128, 109558, 2021.

[9] J.B. Tan, F. Xu, Y.S. Wang and B. Liang. Input Design for Integrated Active Fault Diagnosis and Output Tracking Control, *Automatica*, 142, 110348, 2022. 0348, 2022.

[10] D.M. Raimondo, G.R. Marseglia, R.D. Braatz and J.K. Scott. Fault-tolerant model predictive control with active fault isolation. *The 2nd International Conference on Control and Fault-Tolerant Systems*, pages 444-449, Nice, France, October 9-11, 2013.

[11] H.H. Qiu, F. Xu, B. Liang, and X.Q. Wang. Active fault diagnosis under hybrid bounded and gaussian uncertainties. Automatica, 147:110703, 2023.

[12] J. Wang, X.Y. Lv, Z. Meng and V. Puig. An integrated design method for active fault diagnosis and control. *International Journal of Robust and Nonlinear Control*, DOI:10.1002/rnc.6660, 2023.

Appendix

Proof of Proposition 3.2: It is known that $u_k^{f,c} \oplus H_k^{f,u}\mathbb{B}^{n_u} \subseteq U$. For $H_k^{f,u} \in \mathbb{R}^{n_u \times n_u}$ and $u_k \in u_k^{f,c} \oplus H_k^{f,u}\mathbb{B}^{n_u}$, we have $u_{k,i}^{f,c} - \sum_{j=1}^{n_u} |H_{k,ij}^{f,u}| \leq u_{k,i} \leq u_{k,i}^{f,c} + \sum_{j=1}^{n_u} |H_{k,ij}^{f,u}|$, where $u_{k,i}^{f,c}$ and $u_{k,i}$ are the i-th components of $u_k^{f,c}$ and u_k, respectively, and $H_{k,ij}^{f,u}$ denotes the i-th row and j-th column element of $H_k^{f,u}$. Similarly, for $u_k \in U$, we have $u_i^c - \bar{u}_i \leq u_{k,i} \leq u_i^c + \bar{u}_i$, where u_i^c and $\bar{u}_i$ are the i-th components of u^c and $\bar{u}$, respectively. Furthermore, $u_k^{f,c} \oplus H_k^{f,u}\mathbb{B}^{n_u} \subseteq U$ is transformed into an explicit form:

$$u_{k,i}^{f,c} + \sum_{j=1}^{n_u} |H_{k,ij}^{f,u}| \leq u_i^c + \bar{u}_i, \tag{18a}$$

$$-u_{k,i}^{f,c} + \sum_{j=1}^{n_u} |H_{k,ij}^{f,u}| \leq -u_i^c + \bar{u}_i. \tag{18b}$$

We take (18a) as an example and thus transform (18a) into $u_{k,i}^{f,c} + \mathbf{1}_{1\times n_u}(|H_{k,i}^{f,u}|)^T \leq u_i^c + \bar{u}_i$, where $H_{k,i}^{f,u}$ denotes the i-th row of $H_k^{f,u}$. Furthermore, we can obtain a compact expression $u_k^{f,c} + L(\mathrm{rvec}(|H_k^{f,u}|))^T \leq u^c + \bar{u}$ where $\mathrm{rvec}(|H_k^{f,u}|$ is row vectorization of $|H_k^{f,u}|$. Since $\mathrm{vec}\big((|H_k^{f,u}|)^T\big) = \big(\mathrm{rvec}(|H_k^{f,u}|)\big)^T$ and $\mathrm{vec}(|H_k^{f,u}|) = K_{n_u^2\times n_u^2}\mathrm{vec}\big((|H_k^{f,u}|)^T\big)$ ($K_{n_u^2\times n_u^2}$ is unique and $K_{n_u^2\times n_u^2}^T = K_{n_u^2\times n_u^2}^{-1} = K_{n_u^2\times n_u^2}$). Thus, the inequality is transformed into $u_k^{f,c} + LK_{n_u^2\times n_u^2}\mathrm{vec}(|H_k^{f,u}|) \leq u^c + \bar{u}$. Similarly, (18b) is transformed into $-u_k^{f,c} + LK_{n_u^2\times n_u^2}\mathrm{vec}(|H_k^{f,u}|) \leq -u^c + \bar{u}$. Finally, using ν_k, they are reformulated into (10). ■